Theoretical Chemistry Accounts (2020) 139:42
https://doi.org/10.1007/s00214-019-2528-9

REGULAR ARTICLE

Probing N-heterocyclic olefin as ancillary ligand in scandium-mediated CO_2 to CO conversion

Ana Paula de Lima Batista[1] · **Antonio G. S. de Oliveira-Filho**[1] · **Ataualpa A. C. Braga**[2]

Received: 22 October 2019 / Accepted: 14 December 2019 / Published online: 6 February 2020

Abstract

The transformation of CO_2 to more reactive and value-added chemical species is a crucial way of reducing environmental impact. The $CO_2 + M^+ \rightarrow MO^+ + CO$ reaction, with M = transition metal, is an important channel in gas phase, and it has been accomplished by the Sc^+ species. Besides being a better choice for sustainable transformations, early transition metals, such as scandium, can open new routes for a variety of novel reactions. In this context, DFT calculations are employed to explore N-heterocyclic olefins (NHOs) molecules as a ligand for scandium complexes in the CO_2 to CO reduction. As revealed by the energetics of the process, the described NHO-Sc systems are able to convert CO_2 to CO in an exoergic way, therefore showing great potential for CO_2 conversion.

Keywords CO_2 conversion · Early transition metal complexes · Scandium · NHO ligands · DFT

1 Introduction

The properties and reactions of molecular metal complexes are highly dependent on the ligand and the metal [1–3]. For instance, early transition metals (ETM) are more earth-abundant than late transition metals, such as Ru and Re. Therefore, their mediated reactions tend to be a better choice for sustainable transformations [4, 5]. Besides, the reactivity of ETMs differs from late metals, which opens new routes for a variety of novel reactions [6].

Among the early metal atoms (groups 3–7), scandium is seen as an environmentally benign Lewis acid, and it is compatible with Lewis bases and water [6–8]. For instance, some distinct scandium complexes have been explored in CO_2 activations [6, 9–11]. In particular, the $CO_2 + M^+ \rightarrow MO^+ + CO$ conversion, with M = TM, to CO by metal ions is an important channel in gas-phase, and it has been accomplished by the Sc^+ species [12–15]. The CO product can further be employed for introducing carbonyl functionalities into a plethora of molecular systems, and it is a key component in crucial industrial processes such as the Monsanto/Cativa acetic acid synthesis and the Fischer–Tropsch synthesis of hydrocarbons [16, 17]. Chemical reactions of CO_2 that result in more reactive and value-added chemical species become a crucial way of reducing environmental impact [18–24]. However, due to experimental complications of working with electropositive and small elements, such as scandium ions, the study of CO_2 reactions mediated by their complexes is fairly recent compared to the other ETM systems [6].

To harness the high reactivity of low-valent ETMs toward the activation of small molecules is of great importance [25–30]. Although not usual, stable low-valent scandium complexes, such as the Sc^+ complexes, $[\{\eta^5\text{-}P_3C_2tBu_2)Sc\}_2(\mu\text{-}\eta^6 : \eta^6\text{-}P_3C_3tBu_3)]$ [31],$[Sc(\eta^5\text{-}P_3C_2tBu_2)(\mu\text{-}\eta^2 : \eta^5\text{-}P_3C_2tBu_2)Sc(\eta^5\text{-}P_3C_2tBu_2)]$ [32] and $(LMgBr)_2ScBr$ ($L = Et_2NCH_2CH_2NC(Me)CHC(Me)NCH_2CH_2NEt_2$) [33], have been reported. Others examples of Sc^0 complex and Sc^{2+} complexes [34, 35] are

---

"Festschrift in honor of Prof. Fernando R. Ornellas" Guest Edited by Adélia Justino Aguiar Aquino, Antonio Gustavo Sampaio de Oliveira Filho and Francisco Bolivar Correto Machado.

Electronic supplementary material The online version of this article (https://doi.org/10.1007/s00214-019-2528-9) contains supplementary material, which is available to authorized users.

✉ Ana Paula de Lima Batista
aplima@iq.usp.br

[1] Departamento de Química, Faculdade de Filosofia, Ciências e Letras de Ribeirão Preto, Universidade de São Paulo, Ribeirão Preto, SP 14040-901, Brazil

[2] Departamento de Química Fundamental, Instituto de Química, Universidade de São Paulo, Av. Prof. Lineu Prestes, 748, São Paulo, SP 05508-000, Brazil

also found. For instance, the Sc[N(SiMe$_3$)$_2$]$_3^-$ was described to react with the CO$_2$ molecule [11].

Neutral N-heterocyclic olefins (NHOs), in special, have played a growing role as ligands in transition metal catalysis, mainly because of their pronounced ylidic character [36–42]. Hence, it is expected that NHOs provide extra stabilization to low-valent metal centers such as Sc$^+$ [43–45]. Although other types of N-heterocyclic scandium complexes have been described [6, 9, 10, 46], at the best of our knowledge, none has explored the potential of NHO-scandium (I) compounds toward the CO$_2$ to CO reaction. In particular, the direct influence of NHO ligands on the CO$_2$ to CO conversion mediated by the Sc$^+$. A study that allows us to investigate the sole importance of such ligands, simulating a controlled environment cleared with perturbing factors, provides a direct insight into the molecular or ionic properties of chemically interesting species. Therefore, it offers an ideal way to shed light on mechanistic details of corresponding and more complex condensed-phase systems, i.e., it might reveal the potential of Sc (I) related molecular complexes and their use in CO$_2$ reactions [47–50].

In this context, the present work explores, by means of computational methods, the potential of NHOs as ligand for the scandium(I) mediated reduction of CO$_2$ to CO. Besides, as their structure offers elevated degree of electronic control through the choice of different substituents (R) [2, 39, 43–45, 51–54], we also explore this effect. Figure 1 presents the R groups attached to the current scandium NHOs systems, as well as the nomenclature adopted along with this work.

2 Computational methods

All electronic structure calculations were performed using the Gaussian 09 suite of quantum chemical programs (Revision D0.1) [55]. Geometry optimizations and frequency calculations of all chemical species were performed using the DFT/M06 method [56–58] along with the def2-TZVP basis set [59]. This level of theory is referred as DFT/M06/def2-TZVP along with the work. The M06 density functional showed to be an efficient approach to explore scandium-containing systems [60]. Besides, among other tested density functional methods, it was also able to better reproduce the experimental relative energy of ^{3}Sc$^+$ and ^{1}Sc$^+$ [61, 62]. See the Electronic Supplementary Material for more details. The nature of all structures, as minima or transition states (TSs), was confirmed by the vibrational analysis performed within the harmonic approximation at 298 K and 1 atm. The TSs were identified by only one imaginary frequency mode, which was further followed in order to check the connectivity between the transition state and its corresponding minima.

To analyze the electronic structure and stabilizing effects on the stationary points of the explored potential energy surface (PES), the intrinsic bond orbital (IBO) analyses were carried out using the DFT/PBE/def2-TZVP [59, 63, 64] level of theory, with the univ-JFIT [63] fitting basis set, as implemented in the IboView program [65–67]. Because this program does not have the M06 functional available, the PBE functional was chosen. However, in a previous study [30], we did not find a significant difference between the IBOs computed using PBE and M06 density functionals.

3 Results and discussion

This section is organized as follows: first, a detailed comparison between the ^{1,3}(Sc$^+$) + CO$_2$ PESs is presented. Next, we use the parent NHO system (Scheme 1a) to explore the NHO ligand effect on this conversion. Finally, the influence of selected electron-withdrawing (–CF$_3$ and –CN) and electron-donating substituents (–OMe and –tBu) on the NHO system is also investigated.

3.1 CO$_2$ to CO mechanism mediated by Sc$^+$

As the main point of the current work is to evaluate the influence of the NHO ligand on scandium (I) mediated CO$_2$ to CO reaction, an essential and prior step consists of the analysis of the isolated Sc$^+$ ion mediated conversion. Figure 1 shows the energy profile for this reaction on the singlet (S) and triplet (T) potential energy surfaces.

First of all, we note that the inclusion of the zero-point energy (ZPE) does not change the overall trend along with the reaction. Therefore, in the discussion that follows, we

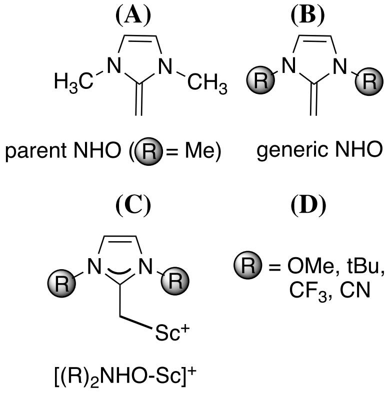

Scheme 1 **a** Parent NHO ligand. **b** General structure of the NHO ligand. **c** General N-heterocyclic olefin scandium(I) complex. **d** Different substituents (R) explored in the CO$_2$ to CO reduction mediated by different NHO-Sc(I) complexes

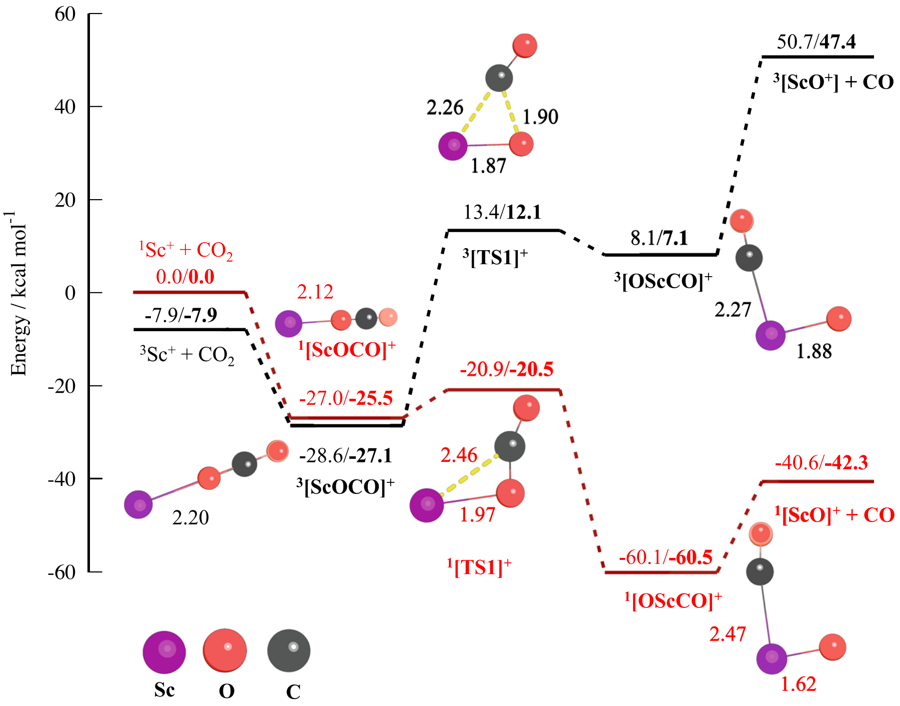

Fig. 1 Singlet (red) and triplet (black) relative energy profiles of the CO_2 to CO mechanism mediated by the Sc^+ ion. All energies are given in kcal mol^{-1} with respect to the separated reactants in their singlet electronic state. Relative energies that do not and do include zero-point energy (ZPE) corrections are written in regular and bold, respectively. Bond distances are in Å

retain ourselves to the electronic energy only. Although the $^1Sc^+$ ion is more energetic than its respective triplet state, the singlet PES offers a way to a more feasible CO_2 to CO reduction mechanism. For instance, at the DFT/M06/def2-TZVP level of theory, the $^1ScO^+ + CO$ channel lies at −40.6 kcal mol^{-1}, while the $^3ScO^+ + CO$ one is at 50.7 kcal mol^{-1}. This result is in agreement with previous studies on the gas-phase $CO_2 \rightarrow CO$ conversion mediated by the Sc^+ ion [12, 13].

The reaction initiates with the formation of the linear $^{1,3}[ScOCO]^+$ form, with the triplet structure only 1.6 kcal mol^{-1} more stable than the singlet one. The singlet and triplet transition states, ^{1,3}[**TS1**], that yield to the $^{1,3}[OScCO]^+$ systems, are −20.9 and 13.4 kcal mol^{-1}, respectively, in the explored energy profiles. Their respective imaginary frequencies are −329.5 and −370.9 cm^{-1}, respectively. The energy required to $^1[ScOCO]^+$ to convert into $^1[OScCO]^+$ is only 6.1 kcal mol^{-1}, while the respective conversion in the triplet PES requires 42.0 kcal mol^{-1}. The singlet $[OScCO]^+$ structure is over 30 kcal mol^{-1} more stable than its related linear one. In the singlet $[OScCO]^+$ intermediate, the ScC bond distance is 2.47 Å, comparatively to 2.27 Å on the triplet $[OScCO]^+$ structure. Therefore, the energy required to dissociate the singlet system into $ScO^+ + CO$ is lower, as viewed in Fig. 1.

Since the singlet PES is the most feasible way to convert CO_2 to CO using Sc^+, all the remaining discussion that follows focus on this multiplicity.

3.2 CO_2 conversion to CO by the parent NHO-Sc(I) complex

Figure 2 shows the minimum energy path (MEP) for the CO_2 to CO reduction mediated by the parent NHO-Sc (I) system. The main point here is to evaluate whether the NHO system has the potential to be used as ligand in larger Sc(I) systems; for instance, if NHO could be a potential ligand in Sc complexes for CO_2 conversions.

As revealed by the energetics of the reaction, the described NHO-Sc (I) system is able to convert CO_2 to CO in an exoergic way. The $[(Me)_2NHO\text{-}ScO]^+ + CO$ channel lies at −30.0 kcal mol^{-1}, i.e., 10.6 kcal mol^{-1} above the corresponding $ScO^+ + CO$ one (Fig. 2, gray line). Therefore, this result raises the potential of NHO systems as ligands for Sc complexes to be employed on the CO_2 to CO reduction. In addition, both intermediates, the linear $[(Me)_2NHO\text{-}ScOCO)]^+$ and the oxidative product $[(Me)_2NHO\text{-}OScCO]^+$ forms, are stable ones (Fig. 2). In the $[(Me)_2NHO\text{-}ScOCO]^+$ system, the Sc-O^2 bond distance is 0.13 Å larger than the corresponding bond in $^1[ScOCO]^+$, which could help to explain the better stabilization of this latter. The transition state $[(Me)_2NHO\text{-}TS1]^+$ (see Fig. 2) that leads to the $[(Me)_2NHO\text{-}OScCO]^+$ intermediate has an imaginary mode of −113.1 cm^{-1} and it is −13.3 kcal mol^{-1} on this potential energy surface. Moreover, since its associated activation energy is only 1.9 kcal mol^{-1}, the process can occur at room temperature.

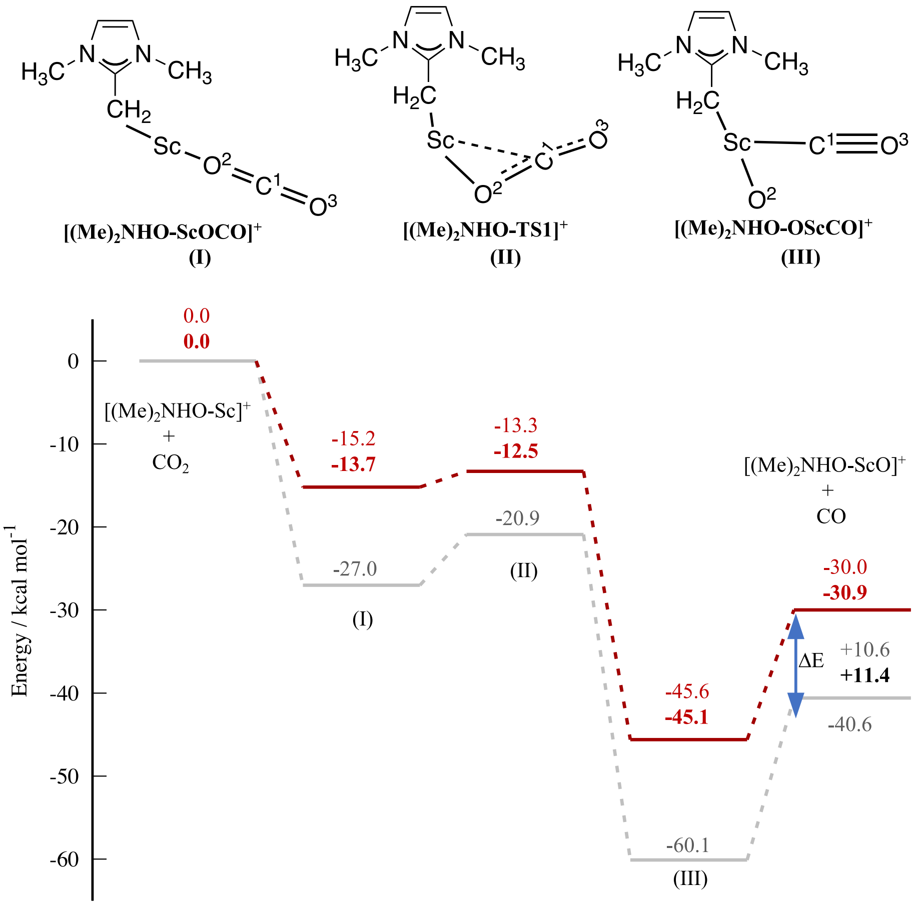

Fig. 2 MEP of the CO_2 to CO reduction mediated by the parent NHO, the [(Me)$_2$NHO-Sc]$^+$ system (red line). The corresponding mechanism mediated by the single Sc^+ ion is also shown for comparison (gray line and gray values). All energies are given in kcal mol^{-1} with respect to the separated reactants. Relative energies that do not and do include zero-point energy (ZPE) corrections are written in regular and bold, respectively

To add a quantitative interpretation to the bond breaking/forming processes and stabilizing effects along with the mechanism, the main active IBOs along with the reaction are also viewed, Fig. 3. IBOs consist of a set of occupied molecular orbitals, which form an exact representation of a given Kohn–Sham wave function.

The analysis over the transition states structures reveals that all five relevant IBOs have contributions upon the formation of the Sc-C^1 bond on the Sc^+ ion mediated mechanism (Fig. 3a), while in the [(Me)$_2$NHO-Sc]$^+$ one, this observation holds true for three of them, IBOs (3), (4) and (5) (Fig. 3b). This result sheds light on the extra stabilization seen on the [**TS1**]$^+$ comparatively to the [(Me)$_2$NHO-TS1]$^+$. The major contributor to this forming process is the IBO (5). IBO (5) starts centered at scandium—it has a d character essentially—on the [(Me)$_2$NHO-ScOCO]$^+$ and $ScOCO^+$ intermediates, and it spreads through the Sc, C^1, O^2 and O^3 atoms on their respective transition states. For more details on the contributions of each atom, see Fig. 3. On the [OScCO]$^+$ and [(Me)$_2$NHO-OScCO]$^+$ intermediates, this IBO remains basically over Sc and O^2 to form a π bond character between them. In addition to this π bond, the Sc and O^2 interaction on the oxidative addition intermediates has great contributions from the IBOs (3) and (4), which show a π and σ character, respectively.

3.3 Substituents effects on the CO_2 conversion

Next, we explore the effect of selected electron-withdrawing (–CF_3 and –CN) and electron-donating substituents (–OMe and –tBu) on the $CO_2 \rightarrow CO$ reduction mediated by the NHO-Sc (I) systems. Figures 4 and 5 present all the corresponding relative energy profiles. The general [(R)$_2$NHO-Sc]$^+$ structures are seen in Scheme 1. The optimized structures of the stationary points discussed below are presented in Electronic Supplementary Material.

Clearly, the CO_2 reduction to CO is a feasible pathway using the NHO-Sc systems, regardless the substituent group. As seen in Figs. 4 and 5, all reactions are exoergic. The linear intermediates, [(tBu)$_2$NHO-ScOCO]$^+$, [(OMe)$_2$NHO-ScOCO]$^+$, [(CF$_3$)$_2$NHO-ScOCO]$^+$ and [(CN)$_2$NHO-ScOCO]$^+$ are well stabilized, −13.7, −19.5, −17.0 and −18.7 kcal mol^{-1}, respectively, in the explored PES. The –tBu substituent provides a [(tBu)$_2$NHO-Sc]$^+$ mediated mechanism energetically similar to its –CH_3 counterpart (Fig. 4a, gray line). This is a reasonable behavior since both are alkyl groups; for instance, the transition states

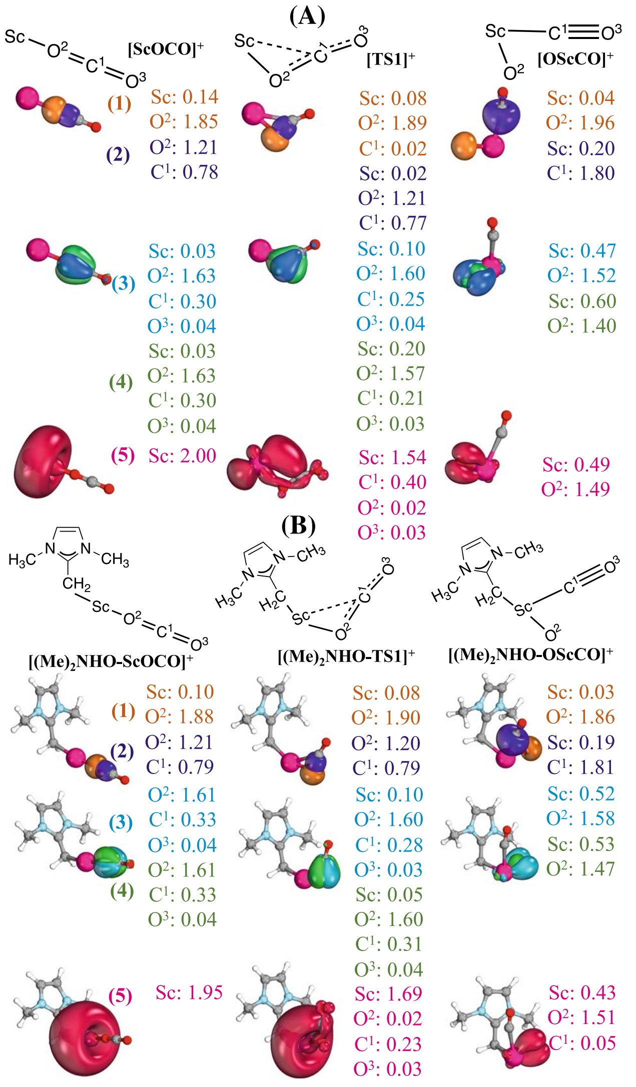

Fig. 3 Relevant IBOs along the reaction mechanism mediated by **a** the Sc^+ ion and **b** the parent $[(Me)_2NHO\text{-}Sc]^+$ complex. Each IBO has a different color. The numbers after the colon are the fraction of electrons assigned to individual atoms of each IBO. The fraction of electrons adds up to two. Some IBOs are plotted together just for convenience

$[(tBu)_2NHO\text{-}TS1]^+$ and $[(Me)_2NHO\text{-}TS1]^+$ are very close in energy, as well as the intermediates $[(tBu)_2NHO\text{-}OScCO]^+$ and $[(Me)_2NHO\text{-}OScCO]^+$. As the electron-donating substituent type is changed, the –OMe group in our case (Fig. 5b), the stabilization along the mediated process is more evident. The transition state $[(OMe)_2NHO\text{-}TS1]^+$ lies at −17.8 kcal mol^{-1} in the current profile, while the oxidative addition intermediate $[(OMe)_2NHO\text{-}OScCO]^+$ is at −50.9 kcal mol^{-1}. The imaginary frequencies associated with the $[(tBu)_2NHO\text{-}TS1]^+$ and $[(OMe)_2NHO\text{-}TS1]^+$ transition states are relatively low, −44.7 and −66.8 cm^{-1}, respectively, as well as their respective activation barriers, 1.0 and 1.7 kcal mol^{-1}.

Within the electron-withdrawing (–CF_3 and –CN) class (Fig. 5), although the transition states $[(CF_3)_2NHO\text{-}TS1]^+$ and $[(CN)_2NHO\text{-}TS1]^+$ have similar energies along their respective mechanism, the –CN substituent offers the largest stabilization to the oxidative addition products, −45.5 kcal mol^{-1} and −53.4 kcal mol^{-1}, respectively, for $[(CF_3)_2NHO\text{-}OScCO]^+$ and $[(CN)_2NHO\text{-}OScCO]^+$. The transition states are characterized by an imaginary frequency of −117.4 cm^{-1} for $[(CF_3)_2NHO\text{-}TS1]^+$ and, −165.9 cm^{-1} for $[(CN)_2NHO\text{-}TS1]^+$; in addition, their activation energies are −2.0 and −3.1 kcal mol^{-1}, respectively. Overall, the electron-withdrawing substituents also make the respective oxidative addition intermediates require less energy to release the CO molecule; for instance, $[(CF_3)_2NHO\text{-}OScCO]^+$ and $[(CN)_2NHO\text{-}OScCO]^+$ require 7.6 kcal mol^{-1} and 12.6 kcal mol^{-1}, respectively, while the $[(OMe)_2NHO\text{-}OScCO]^+$ needs 14.9 kcal mol^{-1}.

4 Conclusions

In the present work, DFT computations were applied to explore the potential of NHOs as a ligand for scandium(I) mediated reduction of CO_2 to CO. The CO_2 to CO mechanism mediated by the $^1Sc^+$ ion was found to be the most feasible way for such conversion. Based on that, the potential of different $^1[NHOs\text{-}Sc]^+$ mediators was also investigated.

As revealed by the energetics of the reaction, the parent NHO-Sc (I) system, the $[(Me)_2NHO\text{-}Sc]^+$ complex, was also able to convert CO_2 to CO in an exoergic way. Therefore, it points out the potential of NHOs ligands for scandium complexes in the CO_2 to CO reduction. Besides, the effect of selected electron-withdrawing (–CF_3 and –CN) and electron-donating (–OMe and –tBu) substituents on the $CO_2 \rightarrow CO$ reduction mediated by the NHOs-Sc (I) systems was also investigated. Regardless of the substituent group, the CO_2 reduction to CO was seen as a viable process by using these NHOs-Sc systems. Among the selected substituents, the –CN group showed to be a better choice for releasing CO more easily. The results discussed along this work raise the potential of the newly NHOs-Sc complexes in CO_2 transformations.

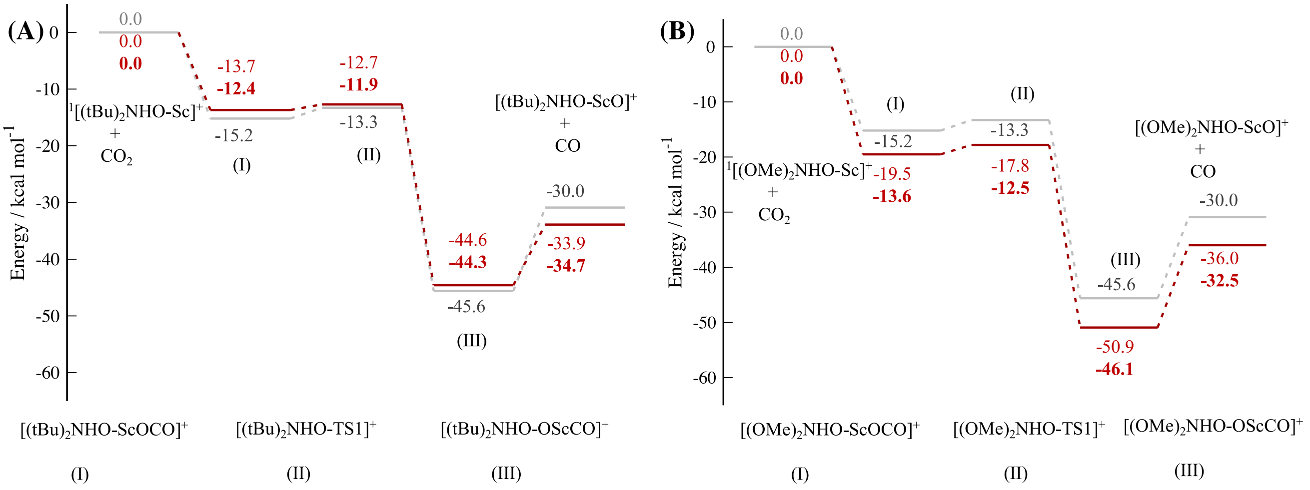

Fig. 4 Relative energy profiles of the CO$_2$ to CO mechanism mediated by different NHO-Sc$^+$ complexes: **a** [(tBu)$_2$NHO-Sc]$^+$ and **b** [(OMe)$_2$NHO-Sc]$^+$. All energies are given in kcal mol^{-1} with respect to the separated reactants. For comparison, the corresponding mechanism mediated by the parent [(Me)$_2$NHO-Sc]$^+$ is also indicated by the gray line and the gray values. Relative energies that do not include and account zero-point energy (ZPE) corrections are written in regular and bold, respectively

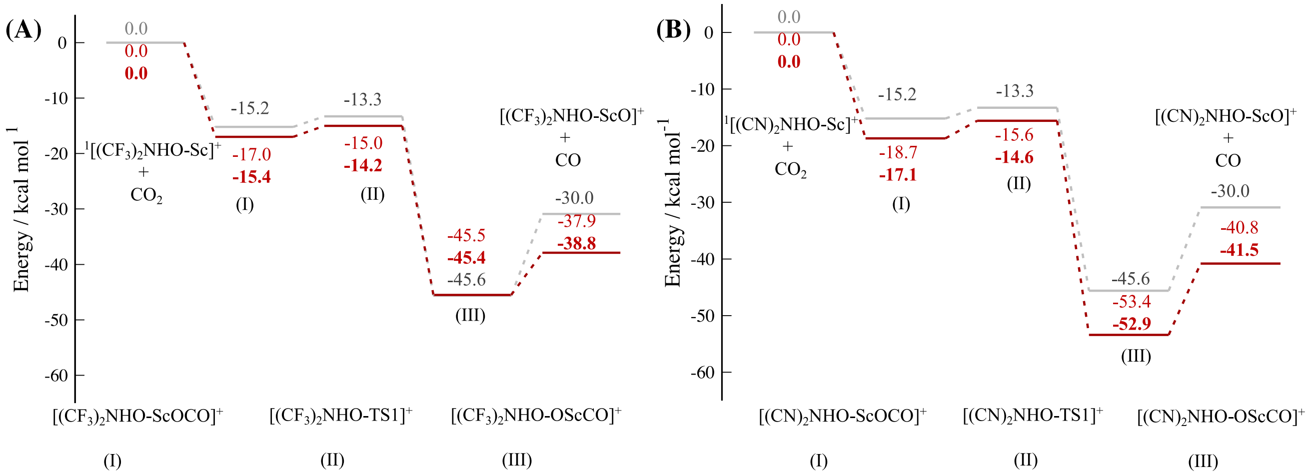

Fig. 5 Relative energy profiles of the CO$_2$ to CO mechanism mediated by different NHO-Sc$^+$ complexes: **a** [(CF$_3$)$_2$NHO-Sc]$^+$ and **b** [(CN)$_2$NHO-Sc]$^+$. All energies are given in kcal mol^{-1} with respect to the separated reactants. For comparison, the corresponding mechanism mediated by the parent [(Me)$_2$NHO-Sc]$^+$ is also indicated by the gray line and the gray values. Relative energies that do not include and account zero-point energy (ZPE) corrections are written in regular and bold, respectively

Acknowledgements A.P.d.L.B., A.G.S.d.O.F and A.A.C.B thank Grants #2017/18238-4, #2015/11714-0, #2014/25770-6 and # 2015/01491-3 from São Paulo Research Foundation (FAPESP), and the support of the High Performance Computing of Universidade de São Paulo (HPC-USP). A.G.S.d.O.F and A.A.C.B also thanks the Conselho Nacional de Desenvolvimento Científico e Tecnológico (CNPq) of Brazil for academic support (Grants #306830/2018-3, #421077/2018-2 and #309715/2017-2). This study was also financed in part by the Coordenação de Aperfeiçoamento de Pessoal de Nível Superior - Brasil (CAPES) - Finance Code 001. The authors also gratefully acknowledge support from FAPESP (Grant No. #2017/11631-2), Shell and the strategic importance of the support given by ANP (Brazil's National Oil, Natural Gas and Biofuels Agency) through the R&D levy regulation.

References

1. Ghadwal RS (2016) Carbon-based two electron σ-donor ligands beyond classical N-heterocyclic carbenes. Dalton Trans 45:16081–16095
2. Durand DJ, Fey N (2019) Computational ligand descriptors for catalyst design. Chem Rev 119:6561–6594
3. Kobayashi K, Tanaka K (2015) Reactivity of CO $_2$ activated on transition metals and sulfur ligands. Inorg Chem 54:5085–5095
4. Chirik P, Morris R (2015) Getting down to earth: the renaissance of catalysis with abundant metals. Acc Chem Res 48:2495–2495
5. Schafer LL, Mountford P, Piers WE (2015) Earth abundant element compounds in homogeneous catalysis. Dalton Trans 44:12027–12028

6. Grice KA (2017) Carbon dioxide reduction with homogenous early transition metal complexes: opportunities and challenges for developing CO_2 catalysis. Coord Chem Rev 336:78–95
7. Kobayashi S, Araki M, Hachiya I (1994) A chiral scandium catalyst for enantioselective Diels–Alder reactions. J Org Chem 59:3758–3759
8. Ogawa C, Kizu K, Shimizu H, Takeuchi M, Kobayashi S (2006) Chiral scandium catalysts for enantioselective Michael reactions of β-Ketoesters. Chem Asian J 1:121–124
9. Arnold PL, Marr IA, Zlatogorsky S, Bellabarba R, Tooze RP (2014) Activation of carbon dioxide and carbon disulfide by a scandium N-heterocyclic carbene complex. Dalton Trans 43:34–37
10. Beh DW, Piers WE, del Rosal I, Maron L, Gelfand BS, Gendy C, Lin J-B (2018) Scandium alkyl and hydride complexes supported by a pentadentate diborate ligand: reactions with CO_2 and N_2O. Dalton Trans 47:13680–13688
11. Woen DH, Chen GP, Ziller JW, Boyle TJ, Furche F, Evans WJ (2017) Solution synthesis, structure, and CO_2 reduction reactivity of a scandium(II) complex, $Sc[N(SiMe_3)_3]^{3-}$. Angew Chem Int 56:2050–2053
12. Sodupe M, Branchadell V, Rosi M, Bauschlicher CW (1997) Theoretical study of M^+-CO_2 and OM^+CO systems for first transition row metal atoms. J Phys Chem A 101:7854–7859
13. Sun Y, Sun X, Huang X (2018) Reaction of CO_2 with atomic transition metal $M^{0,+,-}$ ions: a theoretical study. J Phys Chem A 122:5848–5860
14. Koyanagi GK, Bohme DK (2006) Gas-phase reactions of carbon dioxide with atomic transition-metal and main-group cations: room-temperature kinetics and periodicities in reactivity. J Phys Chem A 110:1232–1241
15. Schwarz H (2017) Metal-mediated activation of carbon dioxide in the gas phase: mechanistic insight derived from a combined experimental/computational approach. Coord Chem Rev 334:112–123
16. Bao J, Yang G, Yoneyama Y, Tsubaki N (2019) Significant advances in C1 catalysis: highly efficient catalysts and catalytic reactions. ACS Catal 9:3026–3053
17. Li J, He Y, Tan L, Zhang P, Peng X, Oruganti A, Yang G, Abe H, Wang Y, Tsubaki N (2018) Integrated tuneable synthesis of liquid fuels via Fischer–Tropsch technology. Nat Catal 1:787–793
18. Wilm LFB, Eder T, Mück-Lichtenfeld C, Mehlmann P, Wünsche M, BuSS F, Dielmann F (2019) Reversible CO_2 fixation by N-heterocyclic imines forming water-stable zwitterionic nitrogen-base-CO_2 adducts. Green Chem 21:640–648
19. Aresta M, Dibenedetto A, Angelini A (2013) The changing paradigm in CO_2 utilization. J CO2 Util 3–4:65–73
20. Aresta M, Dibenedetto A, Quaranta E (2016) State of the art and perspectives in catalytic processes for CO_2 conversion into chemicals and fuels: The distinctive contribution of chemical catalysis and biotechnology. J Catal 343:2–45. Catalytic CO_2 conversion processes to fuels and other small molecules
21. Cuéllar-Franca RM, Azapagic A (2015) Carbon capture, storage and utilisation technologies: a critical analysis and comparison of their life cycle environmental impacts. J CO2 Util 9:82–102
22. Ren Y, Guo C-H, Jia J-F, Wu H-S (2011) A computational study on the chemical fixation of carbon dioxide with epoxide catalyzed by LiBr salt. J Phys Chem A 115:2258–2267
23. Zhao Z, Kong X, Yuan Q, Xie H, Yang D, Zhao J, Fan H, Jiang L (2018) Coordination-induced CO_2 fixation into carbonate by metal oxides. Phys Chem Chem Phys 20:19314–19320
24. Pantazis DA, Tsipis AC, Tsipis CA (2004) Theoretical study on the mechanism of reaction of ground-state Fe atoms with carbon dioxide. Collect Czech Chem Commun 69:13–33
25. Gilbert ZW, Hue RJ, Tonks IA (2015) Catalytic formal [2+2+1] synthesis of pyrroles from alkynes and diazenes via TiII/TiIV redox catalysis. Nat Chem 8:63
26. Chiu H-C, Tonks IA (2018) Trimethylsilyl-protected alkynes as selective cross-coupling partners in titanium-catalyzed [2+2+1] pyrrole synthesis. Angew Chem Int Ed 57:6090–6094
27. Davis-Gilbert ZW, Yao LJ, Tonks IA (2016) Ti-catalyzed multicomponent oxidative carboamination of alkynes with alkenes and diazenes. J Am Chem Soc 138:14570–14573
28. Beaumier EP, Pearce AJ, See XY, Tonks IA (2019) Modern applications of low-valent early transition metals in synthesis and catalysis. Nat Rev Chem 3:15–34
29. Viasus CJ, Alderman NP, Gabidullin B, Gambarotta S (2018) Reaction of CO_2 with a vanadium(II) aryl oxide: synergistic activation of CO_2/oxo groups towards H-atom radical abstraction. Angew Chem 130:11094–11098
30. de Lima Batista AP, de Oliveira-Filho S, Braga AAC (2019) Unveiling the potential of scandium complexes for methane C–H bond activation: a computational study. New J Chem 43:12257–12263
31. Arnold PL, Cloke FGN, Hitchcock PB, Nixon JF (1996) The first example of a formal scandium(I) complex: synthesis and molecular structure of a 22-electron scandium triple decker incorporating the novel 1,3,5-triphosphabenzene ring. J Am Chem Soc 118:7630–7631
32. Clentsmith GKB, Cloke FGN, Green JC, Hanks J, Hitchcock PB, Nixon JF (2003) Stabilization of low-oxidation-state early transition-metal complexes bearing 1,2,4-triphosphacyclopentadienyl ligands: structure of $[Sc(P_3C_2tBu_2)_{22}]$; ScII or mixed oxidation state? Angew Chem Int Ed 42:1038–1041
33. Neculai AM, Neculai D, Roesky HW, Magull J, Baldus M, Andronesi O, Jansen M (2002) Stabilization of a diamagnetic ScIBr molecule in a sandwich-like structure. Organometallics 21:2590–2592
34. Cloke F, Khan K, Perutz R (1991) arene complexes of scandium(0) and scandium(II). J Chem Soc Chem Commun. https://doi.org/10.1039/C39910001372
35. Arnold P, Cloke F, Nixon J (1998) The first stable scandocene: synthesis and characterisation of bis(eta-2,4,5-tri-tert-butyl-1,3-diphosphacyclopentadienyl)scandium(II). Chem Commun 7:797–798
36. Crocker RD, Nguyen TV (2016) The resurgence of the highly ylidic N-heterocyclic olefins as a new class of organocatalysts. Chem Eur J 22:2208–2213
37. Roy MMD, Rivard E (2017) Pushing chemical boundaries with N-heterocyclic olefins (NHOs): from catalysis to main group element chemistry. Acc Chem Res 50:2017–2025
38. Wang Y-B, Wang Y-M, Zhang W-Z, Lu X-B (2013) Fast CO_2 sequestration, activation, and catalytic transformation using N-heterocyclic olefins. J Am Chem Soc 135:11996–12003
39. Naumann S (2019) Synthesis, properties & applications of N-heterocyclic olefins in catalysis. Chem Commun 55:11658–11670
40. Iturmendi A, García N, Jaseer EA, Munárriz J, Sanz Miguel PJ, Polo V, Iglesias M, Oro LA (2016) N-heterocyclic olefins as ancillary ligands in catalysis: a study of their behaviour in transfer hydrogenation reactions. Dalton Trans 45:12835–12845
41. Walther P, Naumann S (2017) N-heterocyclic olefin-based (Co) polymerization of a challenging monomer: homopolymerization of ω-pentadecalactone and its copolymers with γ-butyrolactone, δ-valerolactone, and ϵ-caprolactone. Macromolecules 50:8406–8416
42. Watson IC, Schumann A, Yu H, Davy EC, McDonald R, Ferguson MJ, Hering-Junghans C, Rivard E (2019) N-heterocyclic olefin-ligated palladium(II) complexes as pre-catalysts for Buchwald–Hartwig aminations. Chem Eur J 25:9678–9690
43. Schuldt R, Kästner J, Naumann S (2019) Proton affinities of N-heterocyclic olefins and their implications for organocatalyst design. J Org Chem 84:2209–2218

44. de Lima Batista AP, de Oliveira-Filho AGS, Galembeck SE (2017) CO_2 Sequestration by triazolylidene-derived N-heterocyclic olefins: a computational study. ChemistrySelect 2:4648–4654
45. de Lima Batista AP, de Oliveira-Filho AGS, Galembeck SE (2017) Computationally designed 1,2,4-triazolylidene-derived N-heterocyclic olefins for CO_2 capture, activation, and storage. ACS Omega 2:299–307
46. Pan Y, Xu T, Ge Y-S, Lu X-B (2011) N-heterocyclic carbene scandium complexes: synthesis, structure, and catalytic performance for α-olefin polymerization and copolymerization with 1,5-hexadiene. Organometallics 30:5687–5694
47. Zhou S, Li J, Schlangen M, Schwarz H (2016) Bond activation by metal-carbene complexes in the gas phase. Acc Chem Res 49:494–502
48. Jiang L-X, Zhao C, Li X-N, Chen H, He S-G (2017) Formation of gas-phase formate in thermal reactions of carbon dioxide with diatomic iron hydride Anions. Angew Chem Int 56:4187–4191
49. Hendrickx MFA, Clima S (2006) Electronic structure of the $[MNH_2]^+$ (M=Sc-Cu) complexes. J Phys Chem A 110:12629–12635
50. Sicilia E, Mazzone G, Pérez-González A, Pirillo J, Galano A, Heine T, Russo N (2017) Direct and cluster-assisted dehydrogenation of methane by Nb^+ and Ta^+: a theoretical investigation. Phys Chem Chem Phys 19:16178–16188
51. Dong L, Wen J, Li W (2015) A theoretical investigation of substituent effects on the stability and reactivity of N-heterocyclic olefin carboxylates. Org Biomol Chem 13:8533–8544
52. Saptal VB, Bhanage BM (2016) N-heterocyclic olefins as robust organocatalyst for the chemical conversion of carbon dioxide to value-added chemicals. ChemSusChem 9:1980–1985
53. Denning DM, Falvey DE (2017) Substituent and solvent effects on the stability of N-heterocyclic carbene complexes with CO_2. J Org Chem 82:1552–1557
54. Ajitha MJ, Suresh CH (2012) Assessment of stereoelectronic factors that influence the CO_2 fixation ability of N-heterocyclic carbenes: a DFT study. J Org Chem 77:1087–1094
55. Frisch MJ et al (2009) Gaussian 09 Revision D.01. Gaussian Inc., Wallingford
56. Zhao Y, Truhlar DG (2008) The M06 suite of density functionals for main group thermochemistry, thermochemical kinetics, noncovalent interactions, excited states, and transition elements: two new functionals and systematic testing of four M06-class functionals and 12 other functionals. Theor Chem Acc 120:215–241
57. Hohenberg P, Kohn W (1964) Inhomogeneous electron gas. Phys Rev 136:B864–B871
58. Kohn W, Sham LJ (1965) Self-consistent equations including exchange and correlation effects. Phys Rev 140:A1133
59. Weigend F, Ahlrichs R (2005) Balanced basis sets of split valence, triple zeta valence and quadruple zeta valence quality for H to Rn: design and assessment of accuracy. Phys Chem Chem Phys 7:3297–3305
60. Aoto YA, de Lima Batista AP, Köhn A, de Oliveira-Filho AGS (2017) How to arrive at accurate benchmark values for transition metal compounds: computation or experiment? J Chem Theory Comput 13:5291–5316
61. Kramida A, Yu R, Reader J, NIST ASD Team (2015) NIST atomic spectra database (ver. 5.3), [Online]. http://physics.nist.gov/asd [2019, May 21]. National Institute of Standards and Technology, Gaithersburg, MD
62. Sansonetti J, Martin W, Young S (2015) Handbook of basic atomic spectroscopic data (version 1.1.2). National Institute of Standards and Technology, Gaithersburg, MD. http://physics.nist.gov/Handbook. Accessed 21 May 2019
63. Weigend F (2008) Hartree–Fock exchange fitting basis sets for H to Rn. J Comput Chem 29:167–175
64. Perdew JP, Burke K, Ernzerhof M (1996) Generalized gradient approximation made simple. Phys Rev Lett 77:3865–3868
65. Knizia G (2013) Intrinsic atomic orbitals: an unbiased bridge between quantum theory and chemical concepts. J Chem Theory Comput 9:4834–4843
66. Knizia G, Klein JEMN (2015) Electron flow in reaction mechanisms-revealed from first principles. Angew Chem Int Ed 54:5518–5522
67. Comprido LNS, Klein JEMN, Knizia G, Kastner J, Hashmi ASK (2015) The stabilizing effects in gold carbene complexes. Angew Chem Int Ed 54:10336–10340